IEEE Journal of Microwaves

Received 4 June 2024; revised 30 June 2024; accepted 10 July 2024.

Digital Object Identifier 10.1109/JMW.2024.3427726

A Noninvasive Vein Finder Based on a Tuned Microwave Loop Resonator

SEN BING (Member, IEEE), KHENGDAULIU CHAWANG (Graduate Student Member, IEEE), AND J.-C. CHIAO (Fellow, IEEE)

(Regular Paper)

Electrical and Computer Engineering, Southern Methodist University, Dallas, TX 75205 USA

CORRESPONDING AUTHOR: Sen Bing (e-mail: sbing@smu.edu).

This work was supported in part by the National Science Foundation under Grant ENG-CMMI-1929953, and in part by Mary and Richard Templeton endowment.

This work involved human subjects or animals in its research. Approval of all ethical and experimental procedures and protocols was granted by Southern Methodist University IRB committee Application No. SMU-IRB-22-205.

ABSTRACT In this work, a noninvasive vein finder based on a tuned microwave loop resonator has been demonstrated to locate the vein in a cost-effective, reliable, and convenient way, addressing the challenges in venipuncture, especially in cases of difficult venous access. The sensor is a tuned loop resonator with a radius of 4.7 mm, incorporating a self-tuning pad and operating at 3.25 GHz with a reflection coefficient of −58 dB. It provides localized high-intensity electric fields that penetrate into tissues with sufficient depths. The sensor is based on the detection of electromagnetic resonant frequency shift that is susceptible to the distinctive dielectric properties of blood vessels inside the skin. The extensive simulations and experimental measurements on male and female subjects validate its effectiveness with consistent and distinguishable resonant frequency shifts. The sensor's stability across different forearm locations, its ability to differentiate between arteries and veins, and its adherence to safety regulations with low-power microwave signals contribute to its robustness. It shows great promise for improving venipuncture procedures, reducing complications, and enhancing patient comfort in a low-cost and noninvasive way.

INDEX TERMS Vein finder, noninvasive, impedance matching, electromagnetic wave, RF sensor.

I. INTRODUCTION

Venipuncture is the most common medical procedure applied to obtain blood samples from a vein for clinical investigations [1]. Venipuncture is routinely used for blood donation and blood transfusion to patients [1]. The procedure is invasive and depends on individual phlebotomists' manual operation. Although venipuncture has been a routine procedure in large populations, with an estimated 1.4 billion cases a year in the US reported by the Center for Health Statistics, NHAMCS, in 2016, errors frequently occur. The 2021 National Hospital Ambulatory Care Survey reports that over a quarter (41.8 million) of all emergency department (ED) visits in the US involve the placement of an intravenous (IV) catheter for parenteral fluid administration [2]. Rapidly establishing an IV catheter poses a challenge, especially in patients with difficult venous access (DVA), characterized by a lack of readily visible or palpable veins [3]. Difficult venous access is typically defined as experiencing at least two failed IV attempts [4]. Particularly, first-time intravenous insertion success rates range from 53% to 86% [5], [6], [7], [8], [9], [10], [11], [12], [13], [14], [15] in the pediatric and adult populations. Initial success rates in infants may be even lower at 33% [14], [15]. If failed on the first attempt, the phlebotomist sometimes needs between 2 and 10 attempts to complete the procedure successfully. Reducing the number of venipuncture attempts is a priority in healthcare, given the distressing and painful nature of multiple attempts, such as fainting caused by vasovagal syncope [16], and the associated costs to healthcare [17].

Specific and individual patient factors contribute to insertion failure. Obesity may contribute to challenges in peripheral venous (PV) access, attributed to pathophysiologic changes associated with excess weight. The accumulation of fat in the subcutaneous tissues may result in the presence of

deeply located peripheral veins, posing difficulties in catheterization. This issue of PV access difficulty has been observed in morbidly obese patients in various settings, including in operating rooms and emergency conditions [18], [19], [20]. Age complicates the venipuncture due to the thin and loose skin as well as aging blood vessels [21]. Other factors [4], [6], [10], [11], [12], [13], [22], [23], such as skin colors, diabetes, intravenous drug use, chemotherapy, chronic medical conditions, and needle phobia, could aggravate the difficult venous access. Despite the factors from patients, the shortage of phlebotomists further exacerbates the issue [24], [25]. Sonmez et al. reported that only 38% of 1347 tubes of blood samples were collected by 73 nurses under the safety mechanism [26]. A variety of adverse complications are encountered due to improper site selection and excessive venipuncture caused by the DVA complexity. Hematoma formation is the most common complication of venipuncture [27]. Excessive probing to find the vein is the main reason that causes blood to leak into the tissues, resulting in a bruise. Potentially, it could create fear and phobia in patients with repeated failed venipunctures. Serious cases, including nerve injury, mistaken arterial punctures, thrombus, and syncope, have been reported due to the close distance between the nerves, arterial, and veins [28], [29].

Besides human judgment with the caregiver's visual inspection or touch to palpate the vein with fingers, which is the typical means, several technological approaches have been reported to improve venipuncture success rates [30]. Ultrasound-guided methods are used for locating veins in some reports [22], [31], [32], [33]. However, ultrasound images are noisy, blurry, and sensitive to placement. It requires the vein to be relatively large [34]. Additionally, ultrasound requires expensive equipment and additional trained expertise to obtain meaningful images while simultaneously cannulating the vein [35], making it not universally available. Visible-light transillumination has been utilized to enhance the visualization of veins [36]. Its application has been extended to the varicose vein treatment, as reported in [37]. However, this method necessitates a darkened room, causing inconvenience, and its results have shown inconsistency with instances of burns due to the high intensity of required light [35]. Infrared (IR) imaging emerges as a potential solution due to its deeper penetration into human tissues compared to visible light [38]. Additionally, veins containing deoxygenated hemoglobin-rich blood absorb light significantly at the near-infrared (NIR) wavelengths (740−760 nm) over several centimeters in the tissues. This property is exploited by NIR spectroscopy and can effectively distinguish veins from surrounding tissue [39]. Several commercial devices, such as VeinViewer [40], AccuVein [41], Veinsite [23], and VascuLuminator [42], employ NIR for vascular access procedures. Despite their valuable clinical functions, these NIR devices face limited adoption in clinics due to their high costs, bulky instruments, and user-machine interface. NIR is limited to about a 3-mm depth in tissues, which may not be deep enough as the mean value is 3.1 mm for the basilic veins [43]. These factors prevent them from practical and wide uses as studies have shown no significant benefit by using them compared to manual procedures [44], [45]. Besides, the costs limit their use in economically disadvantaged areas. It is critically important to find a means to locate veins noninvasively, economically, and accurately.

Low-power microwave sensing with nonionizing radiation can be potentially used for vein locating. Nonionizing radiation with a low power density does not present a potential risk of damaging tissues [46]. The dielectric properties of blood vessels are significantly different from those of skin and muscles because of the high water content in the blood plasma. Due to the high contrast in dielectric properties between tissues and vessels, the interactions of electromagnetic fields with different tissues affect wave scattering and provide noninvasive real-time sensing. The presence of veins under the skin can be detected by evaluating the resonant frequency shifts and magnitude changes of reflection coefficients in measurements.

Recent RF devices and integrated circuits are cost-effective with low power consumption. Their sizes can be small and integrated into a wearable device form factor for clinical uses. The advances in electronics make an affordable microwave sensing wearable possible. This work aimed to demonstrate the feasibility of an efficient microwave sensing element that can be conformed to the human forearm to detect the presence of veins under the skin.

II. SENSOR DESIGN AND SIMULATIONS

Compared to waveguides, planar resonators usually have smaller sizes [47], which will be beneficial for the use in vein finding, particularly on children's arms. Resonating cavities [48], [49], [50] are not suitable for comfortably interfacing on the human forearm. Their measurements are limited for media with high dielectric losses [51]. Split ring resonators (SRRs) have found sensing applications in planar circuits [52], [53], [54], [55]. The energy coupling from the outer ring to the inner ring provides the desired resonance. However, the coupling introduces insertion losses, and the two rings bring multiple harmonics, which reduce the quality factor of the resonance of interest. Additionally, both rings are susceptible to environmental changes, particularly concerning wearables. Related to SRR, the complementary split-ring resonator (CSRR) has also been used for microwave sensing [56]. However, CSRRs exhibit higher insertion losses because the inner split ring, responsible for the required resonance, is indirectly excited by the current in the outer ring. This indirect excitation results in a reduced penetration depth of the electric fields into the tissues.

Planar loop resonators seem to be more appropriate, with the advantages of being compact and potentially wearable. However, with the impedance matching issue [46], the poor resonance at the microwave frequencies results in insufficient penetration of fields into tissues. While employing a dynamic

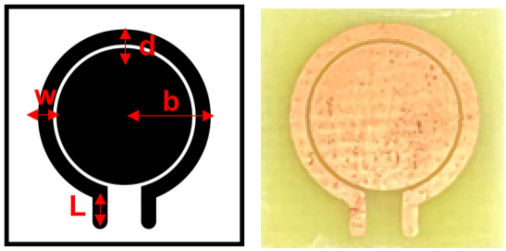

(a) (b)

FIGURE 1. (a) Configuration of the tuned sensor with radius $b = 4.7$ mm, loop width $w = 0.9$ mm, stub length $L = 1.5$ mm, and tuning gap $d = 0.2$ mm. (b) Photograph of the tuned sensor on a FR4 substrate.

matching circuit can potentially achieve a high-quality factor, it results in bulkiness and design limitations. The technical challenge lies in attaining a high-quality factor without compromising the features of being planar and with a small footprint. Our preliminary work [58], [59] developed a self-tuned method for impedance matching in a planar loop resonator by embedding a concentric metal pad, keeping the resonator device architecture simple but efficient. The presence of a center pad provides additional distributed capacitances from the gap between the loop and the metal pad [60] and additional mutual inductance [61] between metal strips across the gap owing to coupled magnetic fields. The gap spacing between the loop and pad tunes the distributed reactance and matches the port impedance at the desired operating frequency. Without changing the overall loop size or adding additional tuning circuits outside of the loop, the resonance of the planar loop can be improved significantly. The loop resonators have been made into compact forms with high resonance performance for near-field sensing. Applications have been investigated for human hydration monitoring [62], [63], [64], [65], subcutaneous implant localization [66], [67], breast cancer detection or imaging [68], [69], [70], and skin cancer distinction [71]. The high-quality factors also enhanced transcutaneous wireless power transfer [72]. In agriculture, the tuned resonator can be used to detect water content percentages of fruits or vegetables [73].

With the advantages that have been verified, this work utilizes a similar tuned loop resonator structure to find the vein under the skin. A rigid substrate capable of withstanding pressure ensures consistent and firm contact with the skin and enhances measurement accuracy. In contrast to our prior use of flexible polyimide substrates, the sensor in this study was designed and fabricated on a rigid single-layer FR4 substrate with a dielectric constant of 4.4 and a thickness of 1.5 mm. The same parameters were used in simulations. The sensor consisted of a loop as the resonating element and a metal pad as the tuning element, as shown in Fig. 1(a). The copper pattern was etched after photolithography was applied. A photo of the resonator is shown in Fig 1(b). The radius of the loop resonator b was 4.7 mm with a connecting stub length $L = 1.5$ mm, which was prepared for a connector to the measurement port. The metal width w was 0.9 mm. The

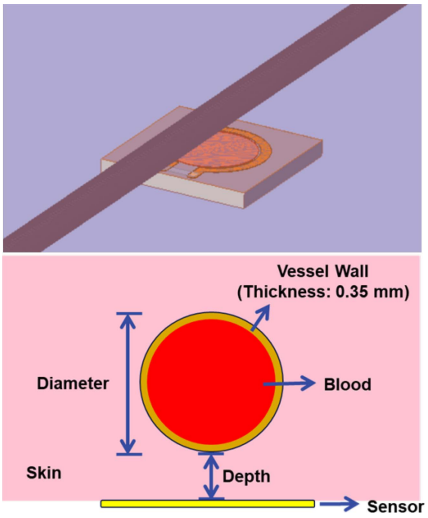

FIGURE 2. Simulation setup: the vein structure consists of a vessel wall and blood.

gap between the loop and the center pad d was chosen to be 0.2 mm, which tuned the resonance below −55.27 dB in a simulation model in which the sensor was placed on the skin with a vein underneath. Fig. 2 shows the simulation. The simulation model consisted of tissues and a single vein. In humans, superficial veins, including cephalic veins (CV) and median cubital veins (MCV), are commonly used for venipuncture [43]. The vein sizes and depths vary per person. According to [43], [74], the average depth range of the vein is 1.7−3 mm, and the average diameter ranges 1.7−4.9 mm. In this work, the simulated vein depth was set at 2 mm with a diameter of 3.6 mm. The vessel wall in the simulation was assumed to be 0.35 mm, according to [75], [76]. The dielectric properties used for skin, blood, and vessel walls were obtained from a documented library in [57], with plots shown in Fig. 3, showing the dielectric constant and conductivity of the three materials between 3 and 4.5 GHz. It should be noted that the database is highly generalized, so discrepancies with measurements on individuals are expected.

Fig. 4 shows the simulated reflection coefficient comparison with and without the vein underneath utilizing the documented data. With a vein underneath, the resonance is at 3.77 GHz with $|s_{11}|$ of −57.27 dB, whereas it is 3.79 GHz with $|s_{11}|$ of −43.52 dB when there is no vein underneath. The robust resonance provides confined electrical fields deep enough to penetrate through the skin and reach the vein, providing sufficient sensitivity to detect the effective permittivities change contributed by the presence of the vein. Fig. 5 shows strong fields across the gap and around the loop. The −10-dB attenuation depth from the surface of the loop, in Fig. 5(b), is 3 mm, covering the vein depth range [43], and the −20-dB attenuation depth is 13 mm. Considering the deep field into the skin, simulations with a vein in a wider range of depths from 1.5 mm to 6 mm were conducted than that of 1.7−3 mm according to [43]. Resonant frequencies are

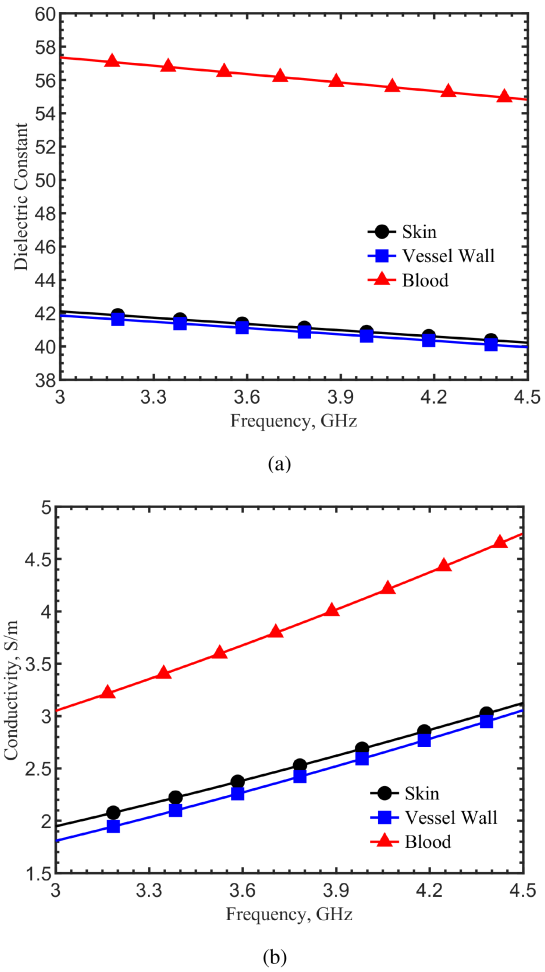

FIGURE 3. Comparison of documented dielectric properties of skin, vessel wall, and blood [57]. (a) Dielectric constant and (b) conductivity.

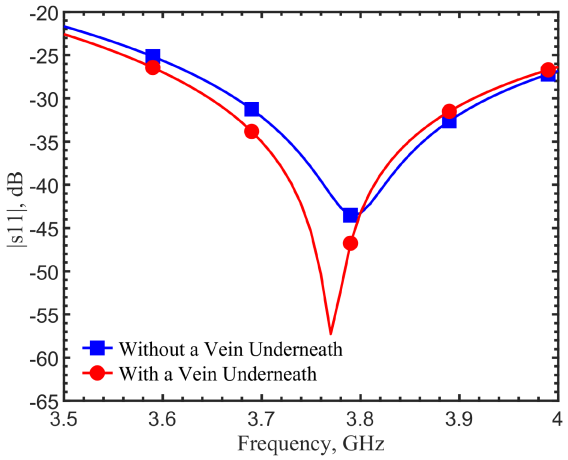

FIGURE 4. Comparison of reflection coefficients for skin with and without a vein underneath.

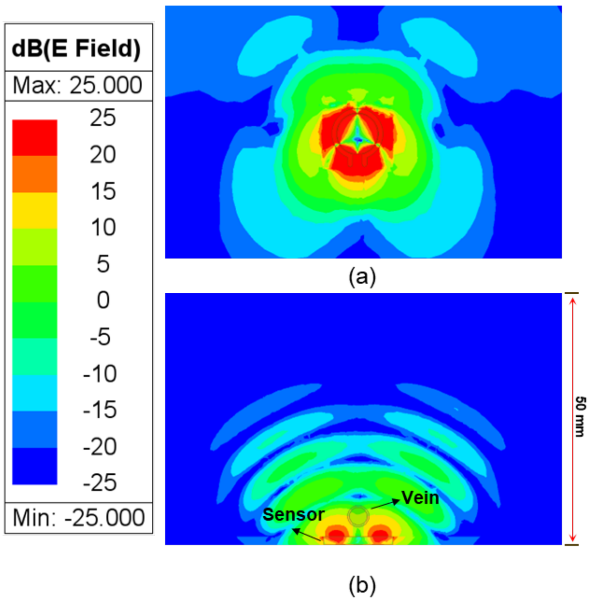

FIGURE 5. Cross sections of electric field distributions from the tuned loop resonator: (a) top view and (b) side view.

compared in Fig. 6 showing the vein can be detectable up to a depth of 6 mm. However, the frequency shift becomes smaller after 3 mm due to the near-field sensor having a maximum field concentrated within the depth of 3 mm, matching the field distribution shown in Fig. 5(b).

III. VEIN DETECTION MEASUREMENTS

A. VEIN DETECTION

The inside of the forearm (antecubital area of the antebrachium) is the most common area for venipuncture. The median cubital vein (MCV) and cephalic vein (CV) are the common targets. The antecubital area skin is relatively thin. The sensor is applied with sufficient pressure onto the forearm skin and connected to a vector network analyzer (Keysight PNA N5227B), as shown in Fig. 7(a) and (b), respectively. Due to the high sensitivity of the tuned sensor, mechanical tension changes on the coaxial cable induce small movements between the arm and cable, causing measurement fluctuations. To improve stability, a laboratory positioning system with bracket mounting is used to stabilize the sensor, as shown in Fig. 7(c). The person can freely move the forearm, allowing the sensor to be placed at different measurement points. The human subjects research protocol ID is SMU-IRB-22-205, approved by the Southern Methodist University IRB committee. According to [77], in vivo dielectric properties are related to genders. Measurements in this work also compare different skins in females and males. Female skin is relatively thinner with a lower dielectric constant compared to male skin before 10 GHz. Similarly, Mayrovitz et al. [78], [79] reported that male skin has a higher tissue dielectric constant than female skin. To investigate skin condition differences with respect to gender, a male and a female subjects of the same age and with similar body sizes were measured on both left and right arms at selected locations with or without clear veins underneath the skin. A commercial near-infrared (NIR) vein finder system

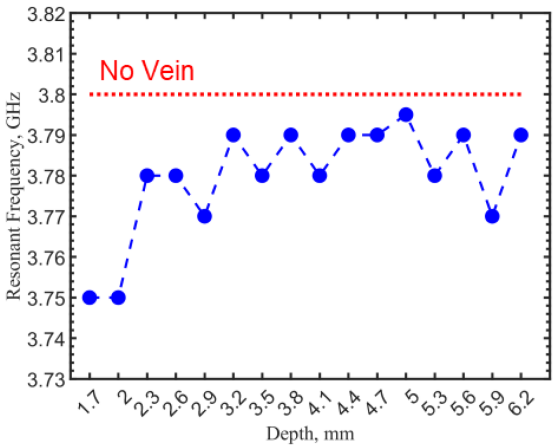

FIGURE 6. Comparison of simulated resonant frequencies with a vein in the depth from 1.7 mm to 6 mm, with a step depth size of 0.3 mm.

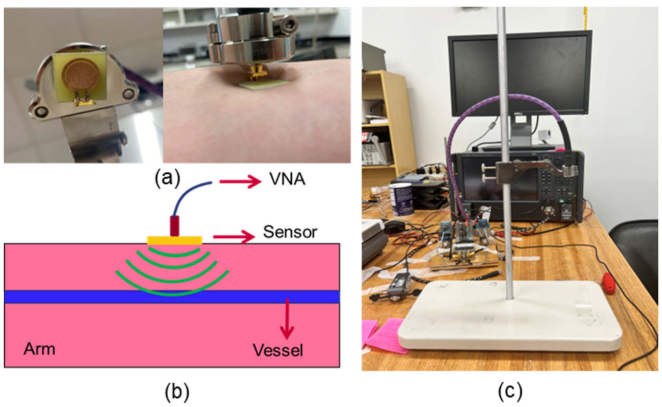

FIGURE 7. (a) Photo of the sensor applied onto the skin in measurements. (b) Setup of measurement. (c) Photo of the positioning system for measurement stabilization.

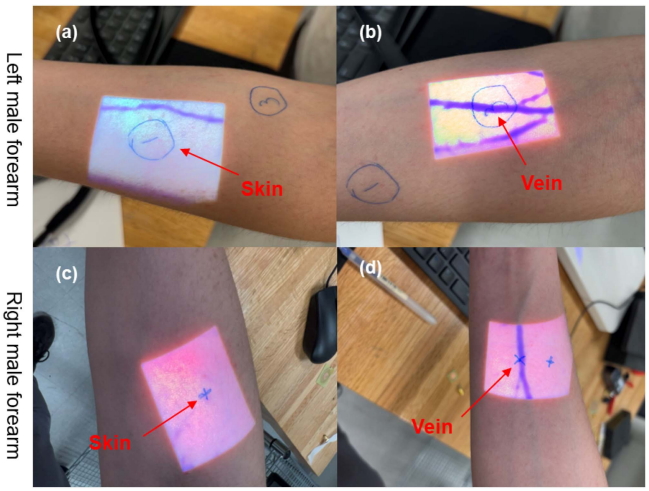

FIGURE 8. Measured locations for skin and skin with veins underneath in the male subject's forearms with the reference of a near-infrared (NIR) imager. (a) Left forearm without a vein underneath in the pen-circled area #1. (b) Left forearm with a vein underneath in the pen-circled area #3. (c) Right forearm without a vein underneath. (d) Right forearm with a vein underneath.

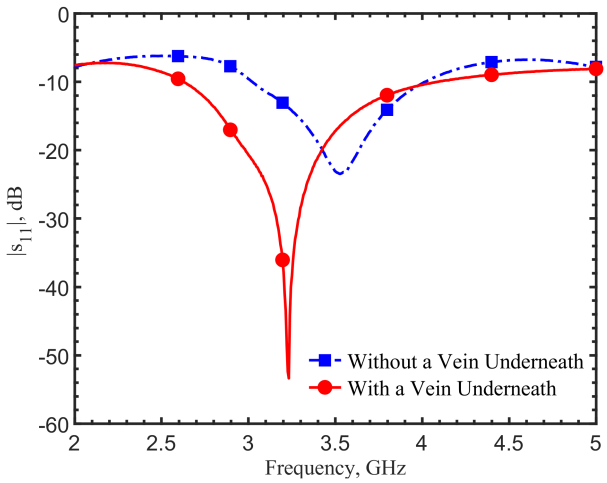

FIGURE 9. Comparison of reflection coefficients in measurements for the skin with and without a vein underneath.

(UMTEC-ZD001, USA) was applied as the reference. Due to the vein locations being different on two forearms and on different persons, the measured physical locations with their distances from the elbows or hands were different. In the male subject's left forearm, two measurement points were selected with the assistance of the NIR finder, with and without a clear vein underneath, as shown in Fig. 8(a) and (b). The circle #1 in the figures on the skin was without a vein and #3 was with a vein. Reflection coefficients are compared in Fig. 9. With a vein underneath, the resonance was 3.232 GHz with $|s_{11}|$ of -53.36 dB, whereas it was 3.527 GHz with $|s_{11}|$ of -23.48 dB when there was no vein underneath. Excellent resonance was expected as the simulation was based on tuning with a vein underneath. The frequency shift was 0.295 GHz.

According to [80] and our observations, the applied contact pressure onto the sensor and skin may affect the $|s_{11}|$. During measurement, even though we intended to control the pressure onto the skin as carefully as possible by the setup, some pressure variations may still exist. The pressure and force applied on the skin compress the internal tissues, squeeze and rearrange relative locations of cells, blood vessels, fat, and water, causing the overall structure changes. This consequentially changes the effective permittivity and conductivity in the tissues, even if the field distribution from the resonator remains the same. Thus, measurements were repeated and recorded five times in each location. Each time, the sensor was removed and placed again in the same location. A verbal confirmation from the subject verified if the person felt the pressure was similar to that in the previous measurement. The resonant frequencies for individual measurements are compared in Fig. 10(a). The measured resonant frequency with the vein underneath was around 3.226 GHz, averaged from five measurements at 3.214, 3.214, 3.226, 3.220, and 3.256 GHz,

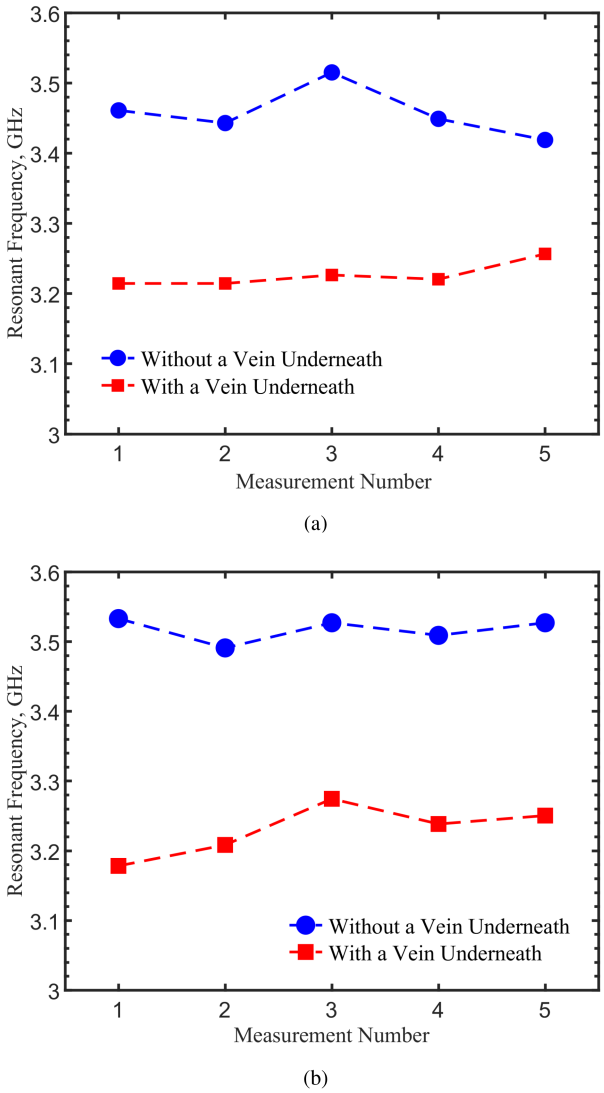

FIGURE 10. **Comparison of measured resonant frequencies for the male subject with and without a vein underneath his forearm skin. Measurements were repeated five times in each location. (a) Left arm and (b) right arm.**

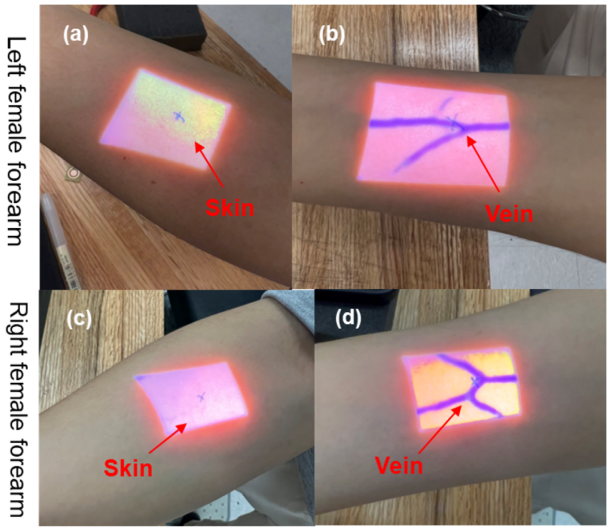

FIGURE 11. **Measured locations for the skin with and without a vein in the female subject's forearms with the reference of the NIR imager. (a) Left forearm without a vein underneath. (b) Left forearm with a vein underneath. (c) Right forearm without a vein underneath and (d) with a vein.**

while the average resonant frequency without a vein underneath was 3.457 GHz from five measurements at 3.461, 3.443, 3.515, 3.449 and 3.419 GHz. The variation ranges were 42 and 96 MHz with and without a vein underneath. Similarly, the measurements were conducted on the right forearm of the same male subject, with and without a vein underneath, as shown in Fig. 8(c) and (d). The measured results are compared in Fig. 10(b). The average resonant frequency was 3.23 GHz with a vein underneath, averaged from five measurements at 3.178, 3.208, 3.275, 3.238, and 3.251 GHz. Without a vein underneath, it was 3.51 GHz, which was averaged from 3.533, 3.491, 3.527, 3.509, and 3.527 GHz. The variation ranges were 96 and 42 MHz with and without a vein underneath. The results were repeatable and distinguishable between the cases with or without a vein underneath in both male subject's forearms. The frequency variations among five measurements in the same location were expected. The frequency variation had an average value of 69 MHz, which was sufficiently small compared to the frequency shift caused by the presence of a vein underneath. An average 259 MHz frequency shift could be found in both forearms when a vein was underneath compared to only the skin.

As for the female subject, measurements were accordingly selected on locations similar to the male subject's on the left and right forearms, as shown in Fig. 11. Measurements were repeated five times in each location for repeatability, and the resonant frequency for each measurement was compared in Fig. 12(a) and (b) for the left and right forearms, respectively. The five measurements in the left forearm with a vein underneath were 3.551, 3.497, 3.575, 3.461, and 3.527 GHz, with an averaged resonant frequency of 3.522 GHz. For the case without a vein underneath, the five measured resonant frequencies were 3.737, 3.768, 3.701, 3.737, and 3.713 GHz, with an average value of 3.731 GHz. The variation ranges were 114 and 66 MHz with and without a vein underneath. In the right forearm of the same female subject, with a vein underneath, the averaged resonant frequency was 3.569 GHz from five measurements at 3.581, 3.599, 3.527, 3.569, and 3.569 GHz, while the one without a vein underneath was 3.736 GHz, which was averaged from 3.816, 3.737, 3.683, 3.695 and 3.749 GHz. The variation ranges were 72 and 13 MHz with and without a vein underneath. The frequency variation was an average value of 96 MHz in the same location. In the measurements on the female subject, there was an average of 188 MHz shift between the cases with and without a vein underneath. The distinguishable frequency shift indicated if there was a vein underneath. Additionally, the overall resonant frequency values, including both with and

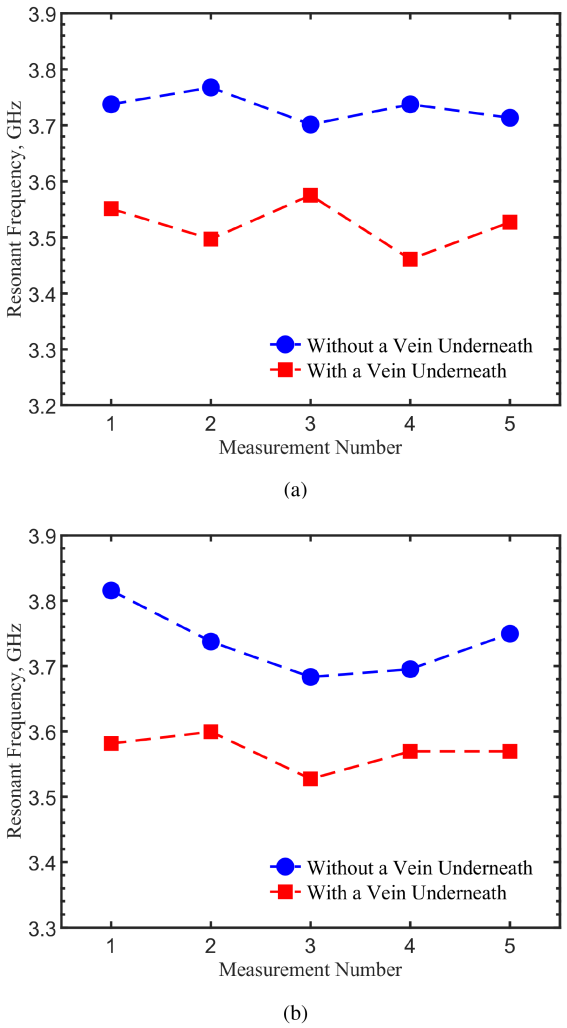

FIGURE 12. Comparison of measured resonant frequencies for the female subject with and without a vein underneath. Measurements were repeated five times in each Location on the (a) left and (b) right forearms.

without a vein underneath, were roughly 200 MHz higher compared to those on the male subject. It was expected because the female skin, with less relative thickness, had a lower tissue dielectric constant, as mentioned earlier in [77], [78], [79], leading to higher resonant frequencies.

B. MEASURED LOCATION EFFECTS

Under the skin, thicknesses of the epidermis, dermis, and hypodermis layers can vary at different locations on the forearm for an individual [81]. The thickness variations lead to variations of effective dielectric properties, causing changes in the measured resonant frequencies. Additionally, the thicknesses of different types of tissues also affect the pressure effects. For example, the compression on the hypodermis/fat layer may vary the tissue thickness more than the epidermis layer. Thus, the body type with thicker layers of fat may experience a larger range of permittivity change when the skin is pressed by the sensor. Differences in curvatures on the forearm for the same person also mean different pressures may be induced on the skin when the sensor is placed. The potential interference factors from curvature, tissue compression and variations of tissue thickness could affect the measurement results. Thus, further investigations were conducted on different measured locations without a vein underneath along the forearm, including the distal, middle, and upper regions of the male subject. The curvature radius and overall skin thickness increase along the forearm from the distal to upper regions. These measurements can be used for calibration to identify the frequency variations without a vein underneath the forearms.

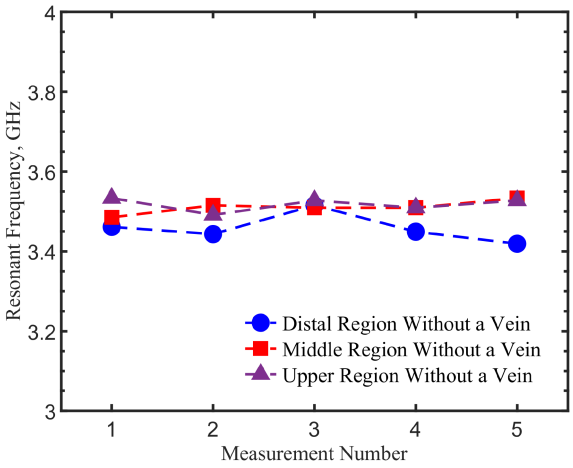

FIGURE 13. Comparison of measured resonant frequencies in various locations on the skin of the forearm, including the distal, middle, and upper regions.

Reflection coefficients for each location were measured five times. Fig. 13 shows the comparison of measured resonant frequencies on the various skin locations. The measured resonant frequencies roughly overlap with the average values of 3.46 GHz, 3.51 GHz, and 3.52 GHz from the distal, middle, and upper regions, respectively. There is a 60 MHz frequency shift, averaged from 5 data, between the distal and upper regions on the forearm. It is almost negligible compared to the frequency shift of around 250 MHz between the cases with and without a vein underneath. This indicated the different measured locations on the forearms did not have a significant effect on detecting the vessels underneath. The distinguishable resonant frequency shift was primarily due to the presence of blood vessels.

C. ARTERY DETECTION

Accidental arterial puncture often results in serious complications and patient distress. It is a prevalent and severe issue for venipuncture [17], [82], [83]. This occurrence is likely when inexperienced caregivers inadvertently mistake an artery for a vein or the distribution of vessels is not clear visually. In some cases, identifying a superficial blood vessel as an artery or vein is not easy, even for an experienced anesthetist [84]. In an emergency situation when antiepileptic drugs can only be administered intravenously for pediatric patients [85], a

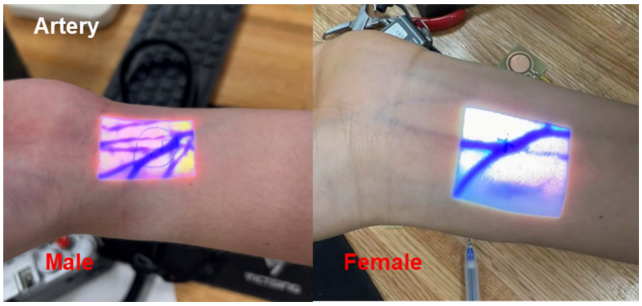

FIGURE 14. Measured locations for arteries in the male and female subjects with the NIR image references.

successful venipuncture for intravenous infusion without arterial puncture is critically important. The radial artery is one of the arteries with the most mistaken arterial punctures [86], [87], especially near the wrist [88], [89], [90], [91]. Thus, the radial artery in the wrist is targeted for measurements in our experiment to investigate if the tuned sensor can distinguish or locate the artery.

The artery, with a larger vessel diameter [88], has higher effective dielectric properties within the sensing field volume from the sensor than veins. Experiments for artery detection were conducted on both male and female subjects. A measured site was selected on the wrist artery in the left forearm for each subject, confirmed with the assistance of the NIR vein finder, as shown in Fig. 14, for both male and female subjects. Measurements were repeated five times in each location. The sensor was removed and placed again on the skin for each measurement. The resonant frequencies at the sites on the same forearm with a vein underneath, with an artery underneath, and without both are compared in Fig. 15(a) and (b) for male and female subjects, respectively. On average, a 192-MHz frequency shift was observed for the male subject between the vein and artery measurements with resonant frequencies of 3.226 GHz and 3.034 GHz. An average 423-MHz frequency shift between 3.457 GHz and 3.034 GHz for skin and artery measurements for male. For the female subject, it was 220 MHz between 3.522 GHz and 3.302 GHz for vein and artery measurements, while a 429-MHz frequency shift between 3.731 GHz and 3.302 GHz for the skin and artery measurements. Based on different resonant frequency shifts compared to skin measurements, the results indicate that the tuned sensor can distinguish arteries and veins from the skin. The result showed the feasibility of avoiding mistaken arterial punctures.

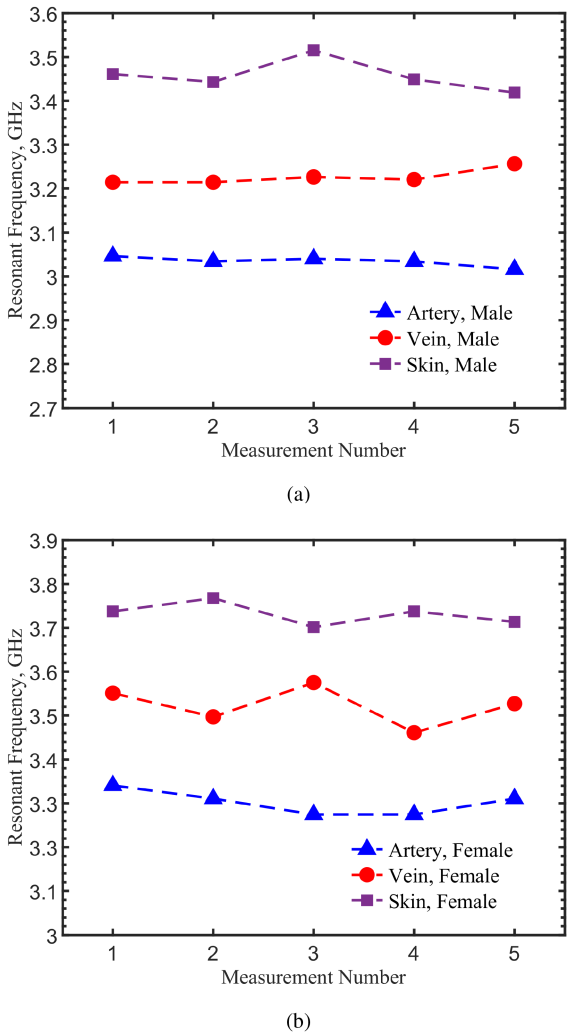

FIGURE 15. Comparison of measured resonant frequencies for the skin, vein, and artery. Measurements were repeated five times in each measured location on the (a) male and (b) female subjects.

IV. DISCUSSION

A. EXPOSURE SAFETY

Considering the sensor on the skin radiates electrical fields into the tissues, the electromagnetic exposure safety concern should be evaluated. While it emits non-ionizing radiation without a worry for molecular changes or DNA damages that could harm biological tissues like X-rays or gamma rays [92], it has been known that high levels of RF radiation exposure may still pose health risks [93]. The rapid heating of biological tissues by RF energy has been linked to potential harm. Federal Communications Commission (FCC) mandates compliance with a Specific Absorption Rate (SAR) level of 1.6 watts per kilogram (W/kg) that is averaged over one gram of tissues [94]. The ICNIRP guidelines specify a limit of 2 W/kg averaged over 10 grams of tissues [95]. To investigate the SAR from the tuned sensor on the skin, simulations were conducted. The input power from the source was set at −5 dBm, the same as the PNA setting in the measurements. The SAR field distributions in 2-D cross-sections inside the tissues without a vein underneath are shown in Fig. 16(a) and (b) as the top and side views, respectively, while Fig. 16(c) and (d) show the top and side views with a vein underneath. The vein diameter is 3 mm. The SAR levels have a maximum value of 0.07 W/kg at the resonant frequency of 3.375 GHz without a vein underneath and 0.08 W/kg at 3.375 GHz without a vein underneath. The SAR levels in both cases are far below the limits of 1.6 W/kg and 2 W/kg defined by FCC and

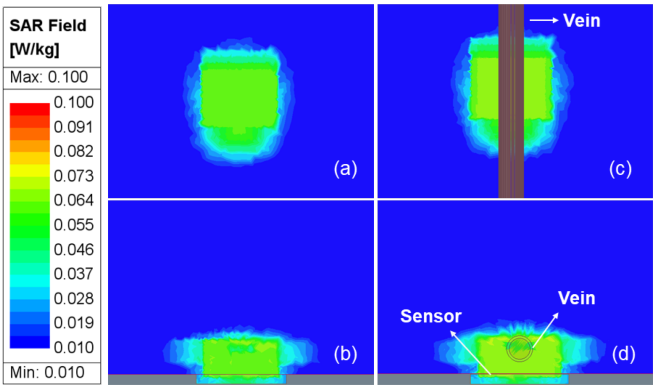

FIGURE 16. Cross sections showing SAR field distributions from the tuned loop resonator. (a) Top and (b) side views without a vein underneath. (c) Top and (d) side views with a vein underneath the skin.

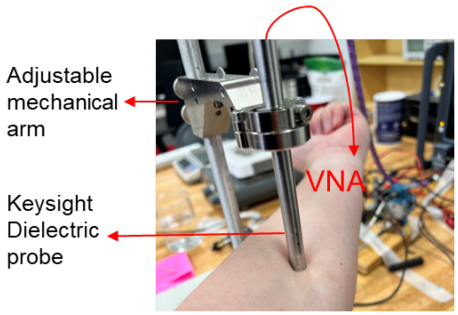

FIGURE 17. Setup of skin dielectric properties measurement using the dielectric probe kit.

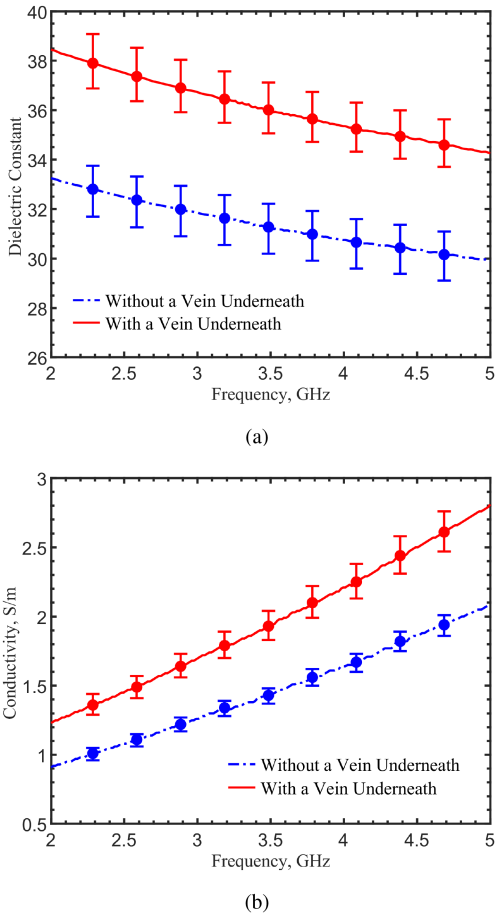

FIGURE 18. Comparison of measured dielectric properties of skin with and without a vein underneath. (a) Dielectric constant and (b) conductivity.

ICNIRP. Therefore, the proposed sensors should be safe from electromagnetic field exposure. The field distributions show that the energy does not penetrate through the forearm and is limited in localized areas. Thus, there should not be a concern about the energy affecting other organs in the body.

B. DIELECTRIC PROPERTY MEASUREMENTS

The repeatable results in Section III manifest that skin with a vein underneath has a higher effective permittivity, which matches the theory as blood vessels contain higher water content than cells. To the best of our knowledge, there was no study that compares effective dielectric properties on the skin with or without veins underneath. The theory and simulation conducted in this study were based on the documented dielectric properties of the skin, blood, and blood vessel wall in [57]. The documented data were averaged from multiple values obtained from separated or biopsied samples that might not resemble the effective dielectric properties on the skin. The samples were individualized, which meant they were not integrated into a single living structure and without circulating water/blood in them.

To further investigate our theory, direct measurements of dielectric properties on the human forearm were conducted using a coaxial probe kit (Keysight N1501 A). This measurement will provide effective dielectric properties of the connected tissues in the matrices under the skin instead of separated samples from biopsies. The probe was placed on the skin of the male's forearm with and without a vein underneath, as shown in Fig. 17. The measured sites were the same as those for the resonator sensor and validated by the NIR vein finder shown in Fig. 8(a) and (b). The measured dielectric constant and conductivity are shown in Fig. 18(a) and (b). The error bars show the data ranges from five measurements. It was observed that the pressures on the skin affected the measurement results due to the changes in the vein depths caused by the pressure and compression of tissues, although the probe was pushed lightly on the skin with the intention of minimizing the data deviations from various pressures. The differences in the effective dielectric properties between the ones with and without veins underneath were distinguishable. The measured site with a vein underneath has a higher effective dielectric constant and conductivity, as expected, due to the high water content within the vein, resulting in a lower resonant frequency when our sensor is applied.

There are clear discrepancies between the documented dielectric properties from the biopsied samples [57], shown in Fig. 3(a) and (b), and the measured results on the skin,

shown in Fig. 18(a) and (b). Several factors need to be considered. First, the biopsied samples only represented individual tissue properties. These samples were not the same as they were in realistic physiological conditions. Second, the values presented in [57] were calculated as averaged values sampled from various subjects. The individual persons' conditions were unknown. The tissue compositions in individuals could play an important role in affecting these tissues' dielectric properties. Third, the samples were individualized during the microwave measurements. It is unclear if the fields from the measurements were confined within the sample and isolated from environmental effects.

The effective dielectric properties in the measurement volume are influenced by the tissue composition and also the field distributions from the probe. The variations from above mentioned effects seem to be limitless. Furthermore, in the measurements of using a coaxial probe to evaluate the effective dielectric properties, although they give a holistic view into the connected tissues, the results are person-dependent. From Fig. 18, the average effective dielectric constants were 36.72−34.83 in the range of 3−4.5 GHz for the skin with a vein underneath, as compared to 57.36−54.82 for blood and 42.12−40.23 for the skin in Fig. 3. However, the average effective dielectric constants were 31.84−30.36 in the range of 3−4.5 GHz for the skin without a vein underneath, which was lower than 42.12−40.23 for the skin in Fig. 3. The variation in tissue composition, including fat layers and their thickness, capillary blood vessel densities, water content in cells and epidermis layer thickness, could affect the overall effective dielectric constants. As these factors are person-dependent and it is difficult to design a sensing device that relies on deterministic permittivity and conductivity inside the tissues, this highlights the feature of sensing the differences across the skin surface to identify the vein location. The high-quality factor resonator, together with the distinguishable difference for the skin with and without a vein underneath in Fig. 18, makes this detection possible without the necessity of knowing the accurate values of dielectric properties in individuals.

V. CONCLUSION

This work demonstrated a novel noninvasive vein finder based on a tuned microwave loop resonator. It provides potentially a low-cost, reliable, and convenient solution to address the persistent challenges in venipuncture, especially for the cases of difficult venous access. The planar loop resonator tuned with a metal pad ensures a compact design suitable for wearables and provides a high-quality factor of resonance for high sensitivity to detect permittivity changes due to the existence of veins under the skin. The utilization of low-power microwave sensing on the distinctive dielectric properties between blood vessels and tissues provides a high level of sensitivity and specificity.

Extensive simulations and experimental measurements on male and female subjects confirm the sensor's ability to detect veins with consistently distinguishable resonant frequency shifts. The repeatability across different forearm locations was validated. The capability to differentiate between arteries and veins demonstrates the robustness and potential to improve venipuncture procedures, reduce complications, and enhance patient comfort. Safety considerations for specific absorption rates are addressed by simulations showing they are below regulatory limits. Furthermore, direct measurements of dielectric properties on human forearms, which have not been documented before, validate the principle. This work verifies the capability and performance of noninvasive detection of vein locations by a planar loop resonator on the skin of the forearm. The validation is performed with a vector network analyzer to ensure accuracy. The next step will be the development of an electronic system for detecting and locking the resonance frequencies of interest when the sensor is placed on the skin.

REFERENCES

[1] World Health Organization, "WHO guidelines on drawing blood: Best practices in phlebotomy," 2010. [Online]. Available: http://www.who.int/iris/handle/10665/44294

[2] C. Cairns and K. Kang, "National hospital ambulatory medical care survey: 2021 emergency department summary tables," Tech. Rep., 2021. [Online]. Available: https://ftp.cdc.gov/pub/Health_Statistics/NCHS/Dataset_Documentation/NHAMCS/doc21-ed-508.pdf

[3] L. L. Kuensting, S. DeBoer, R. Holleran, B. L. Shultz, R. A. Steinmann, and J. Venella, "Difficult venous access in children: Taking control," *J. Emerg. Nurs.*, vol. 35, no. 5, pp. 419–424, Sep. 2009.

[4] J. M. Fields, N. E. Piela, A. K. Au, and B. S. Ku, "Risk factors associated with difficult venous access in adult ed patients," *Amer. J. Emerg. Med.*, vol. 32, no. 10, pp. 1179–1182, Oct. 2014.

[5] P. J. Carr, J. C. R. Rippey, C. A. Budgeon, M. L. Cooke, N. Higgins, and C. M. Rickard, "Insertion of peripheral intravenous cannulae in the emergency department: Factors associated with first-time insertion success," *J. Vasc. Access*, vol. 17, no. 2, pp. 182–190, Mar. 2016.

[6] N. J. Cuper, J. C. de Graaff, A. T. H. van Dijk, R. M. Verdaasdonk, D. B. M. van der Werff, and C. J. Kalkman, "Predictive factors for difficult intravenous cannulation in pediatric patients at a tertiary pediatric hospital," *Pediatr. Anesth.*, vol. 22, no. 3, pp. 223–229, Mar. 2012.

[7] A. F. Jacobson and E. H. Winslow, "Variables influencing intravenous catheter insertion difficulty and failure: An analysis of 339 intravenous catheter insertions," *Heart Lung*, vol. 34, no. 5, pp. 345–359, Sep. 2005.

[8] A. F. Jacobson, "Intradermal normal saline solution, self-selected music, and insertion difficulty effects on intravenous insertion pain," *Heart Lung*, vol. 28, no. 2, pp. 114–122, Mar. 1999.

[9] F. Lapostolle et al., "Prospective evaluation of peripheral venous access difficulty in emergency care," *Intensive Care Med.*, vol. 33, no. 8, pp. 1452–1457, Aug. 2007.

[10] M. O'Neill, M. Dillane, and N. F. Hanipah, "Validating the difficult intravenous access clinical prediction rule," *Pediatr. Emerg. Care*, vol. 28, no. 12, pp. 1314–1316, Dec. 2012.

[11] M. W. Riker, C. Kennedy, B. S. Winfrey, K. Yen, and M. D. Dowd, "Validation and refinement of the difficult intravenous access score: A clinical prediction rule for identifying children with difficult intravenous access," *Academic Emerg. Med.*, vol. 18, no. 11, pp. 1129–1134, Nov. 2011.

[12] M. D. Witting, "IV access difficulty: Incidence and delays in an urban emergency department," *J. Emerg. Med.*, vol. 42, no. 4, pp. 483–487, Apr. 2012.

[13] K. Yen, A. Riegert, and M. Gorelick, "Derivation of the diva score: A clinical prediction rule for the identification of children with difficult intravenous access," *Pediatr. Emerg. Care*, vol. 24, no. 3, pp. 143–147, Mar. 2008.

[14] R. A. Lininger, "Pediatric peripheral i.v. insertion success rates," *Pediatr. Nurs.*, vol. 29, no. 5, pp. 351–354, Sep. 2003.

[15] K. Black, M. Pusic, D. Harmidy, and D. McGillivray, "Pediatric intravenous insertion in the emergency department: Bevel up or bevel down?," *Pediatr. Emerg. Care*, vol. 21, no. 11, pp. 707–711, Nov. 2005.

[16] P. T. Gilchrist and B. Ditto, "The effects of blood-draw and injection stimuli on the vasovagal response," *Psychophysiol.*, vol. 49, no. 6, pp. 815–820, Jun. 2012.

[17] N. L. Moureau et al., "Vessel health and preservation (Part 1): A new evidence-based approach to vascular access selection and management," *J. Vasc. Access*, vol. 13, no. 3, pp. 351–356, Jul. 2012.

[18] C. Jbeili et al., "Out-of-hospital management characteristics of severe obese patients," *Annales Françaises d'anesthésie et de Réanimation*, vol. 26, no. 11, pp. 921–926, Nov. 2007.

[19] P. Juvin, A. Blarel, F. Bruno, and J.-M. Desmonts, "Is peripheral line placement more difficult in obese than in lean patients?," *Anesth. Analg.*, vol. 96, no. 4, p. 1218, Apr. 2003.

[20] O. O. Nafiu, C. Burke, A. Cowan, N. Tutuo, S. Maclean, and K. K. Tremper, "Comparing peripheral venous access between obese and normal weight children," *Pediatr. Anesth.*, vol. 20, no. 2, pp. 172–176, Feb. 2010.

[21] L. Dougherty, "Intravenous therapy in older patients," *Nurs. Standard*, vol. 28, no. 6, pp. 50–58, Oct. 2013.

[22] L. Brannam, M. Blaivas, M. Lyon, and M. Flake, "Emergency nurses' utilization of ultrasound guidance for placement of peripheral intravenous lines in difficult-access patients," *Academic Emerg. Med.*, vol. 11, no. 12, pp. 1361–1363, Dec. 2004.

[23] F. B. Chiao et al., "Vein visualization: Patient characteristic factors and efficacy of a new infrared vein finder technology," *Brit. J. Anaesth.*, vol. 110, no. 6, pp. 966–971, Jun. 2013.

[24] P. Larsen et al., "Pediatric peripheral intravenous access: Does nursing experience and competence really make a difference?," *J. Infusion Nurs.*, vol. 33, no. 4, pp. 226–235, Jul. 2010.

[25] D. Millam and L. Hadaway, "On the road to successful IV starts," *Nursing*, vol. 30, pp. 34–48, May 2000.

[26] C. Sonmez, U. Yıldız, N. Akkaya, and F. Taneli, "Preanalytical phase errors: Experience of a central laboratory," *Cureus*, vol. 12, no. 3, Mar. 2020, Art. no. e7335.

[27] O. Y. Buowari, "Complications of venepuncture," *Adv. Biosci. Biotechnol.*, vol. 4, no. 1, pp. 126–128, 2013.

[28] R. Serra et al., "Adverse complications of venipuncture: A systematic review," *Acta Phlebologica*, vol. 19, no. 1, pp. 11–15, Apr. 2018.

[29] H. J. Galena, "Complications occurring from diagnostic venipuncture," *J. Fam. Pract.*, vol. 34, no. 5, pp. 582–584, 1992.

[30] A. Sabri, J. Szalas, K. S. Holmes, L. Labib, and T. Mussivand, "Failed attempts and improvement strategies in peripheral intravenous catheterization," *Bio-Med. Mater. Eng.*, vol. 23, no. 1/2, pp. 93–108, 2013.

[31] B. C. Md, S. T. Md, and G. W. H. Md, "Predictors of success in nurse-performed ultrasound-guided cannulation," *J. Emerg. Med.*, vol. 33, no. 4, pp. 401–405, Nov. 2007.

[32] N. L. Panebianco, J. M. Fredette, D. Szyld, E. B. Sagalyn, J. M. Pines, and A. J. Dean, "What you see (sonographically) is what you get: Vein and patient characteristics associated with successful ultrasound-guided peripheral intravenous placement in patients with difficult access," *Academic Emerg. Med.*, vol. 16, no. 12, pp. 1298–1303, Dec. 2009.

[33] T. G. Costantino, A. K. Parikh, W. A. Satz, and J. P. Fojtik, "Ultrasonography-guided peripheral intravenous access versus traditional approaches in patients with difficult intravenous access," *Ann. Emerg. Med.*, vol. 46, no. 5, pp. 456–461, Nov. 2005.

[34] J. S. Donaldson, F. P. Morello, J. J. Junewick, J. C. O'Donovan, and J. Lim-Dunham, "Peripherally inserted central venous catheters: US-guided vascular access in pediatric patients," *Radiology*, vol. 197, no. 2, pp. 542–544, Nov. 1995.

[35] V. P. Zharov, S. Ferguson, J. F. Eidt, P. C. Howard, L. M. Fink, and M. Waner, "Infrared imaging of subcutaneous veins," *Lasers Surg. Med.*, vol. 34, no. 1, pp. 56–61, Jan. 2004.

[36] R. A. Weiss and M. P. Goldman, "Transillumination mapping prior to ambulatory phlebectomy," *Dermatol. Surg.*, vol. 24, no. 4, pp. 447–450, Apr. 1998.

[37] R. W. Franz, J. F. Hartman, and M. L. Wright, "Treatment of varicose veins by transilluminated powered phlebectomy surgery: A 9-year experience," *Int. J. Angiol.*, vol. 21, no. 4, pp. 201–208, Dec. 2012.

[38] H. Haxthausen, "Infrared photography of subcutaneous veins: Demonstration of concealed varices in ulcer and eczema of the leg," *Brit. J. Dermatol.*, vol. 45, no. 12, pp. 506–511, Jan. 1933.

[39] A. Roggan, M. Friebel, K. Dörschel, A. Hahn, and G. Müller, "Optical properties of circulating human blood in the wavelength range 400-2500 nm," *J. Biomed. Opt.*, vol. 4, no. 1, pp. 36–46, Jan. 1999.

[40] L. L. Chapman, B. Sullivan, A. L. Pacheco, C. P. Draleau, and B. M. Becker, "Veinviewer-assisted intravenous catheter placement in a pediatric emergency department," *Academic Emerg. Med.*, vol. 18, no. 9, pp. 966–971, Sep. 2011.

[41] Accuvein vein visualization system. Accessed: Mar. 2024. [Online]. Available: https://www.accuvein.com/vein-visualization-system/

[42] N. J. Cuper et al., "Visualizing veins with near-infrared light to facilitate blood withdrawal in children," *Clin. Pediatrics*, vol. 50, no. 6, pp. 508–512, Jun. 2011.

[43] K. Mukai et al., "Safety of venipuncture sites at the cubital fossa as assessed by ultrasonography," *J. Patient Saf.*, vol. 16, no. 1, pp. 98–105, Mar. 2020.

[44] S. J. Curtis, W. R. Craig, E. Logue, B. Vandermeer, A. Hanson, and T. Klassen, "Ultrasound or near-infrared vascular imaging to guide peripheral intravenous catheterization in children: A pragmatic randomized controlled trial," *Can. Med. Assoc. J.*, vol. 187, no. 8, pp. 563–570, May 2015.

[45] J. M. Leipheimer et al., "First-in-human evaluation of a hand-held automated venipuncture device for rapid venous blood draws," *Technology*, vol. 7, no. 3/4, pp. 98–107, Sep. 2019.

[46] J.-C. Chiao et al., "Applications of microwaves in medicine," *IEEE J. Microwaves*, vol. 3, no. 1, pp. 134–169, Jan. 2023.

[47] J.-C. Chiao, S. Bing, and K. Chawang, "Review on noninvasive radiofrequency sensing for closed-loop body health management," in *Proc. IEEE Int. Symp. Radio-Freq. Integr. Technol.*, Piscataway, Aug. 2021, pp. 1–3.

[48] M. P. Robinson, J. Clegg, and D. A. Stone, "A novel method of studying total body water content using a resonant cavity: Experiments and numerical simulation," *Phys. Med. Biol.*, vol. 48, no. 1, pp. 113–125, Jan. 2003.

[49] D. A. Stone and M. P. Robinsons, "Total body water content observations using cavity - Perturbation techniques," in *Proc. IEEE High Freq. Postgraduate Student Colloq.*, 2003, pp. 31–34.

[50] A. W. Kraszewski, S. O. Nelson, and T. S. You, "Use of a microwave cavity for sensing dielectric properties of arbitrarily shaped biological objects," *IEEE Trans. Microw. Theory Techn.*, vol. 38, no. 7, pp. 858–863, Jul. 1990.

[51] M. S. Venkatesh and G. S. V. Raghavan, "Overview of dielectric properties measuring techniques," *Can. Biosyst. Eng.*, vol. 47, pp. 15–30, 2005.

[52] K. Aydin, I. Bulu, K. Guven, M. Kafesaki, C. M. Soukoulis, and E. Ozbay, "Investigation of magnetic resonances for different split-ring resonator parameters and designs," *New J. Phys.*, vol. 7, no. 1, 2005, Art. no. 168.

[53] M. Baghelani, Z. Abbasi, M. Daneshmand, and P. E. Light, "Non-invasive continuous-time glucose monitoring system using a chipless printable sensor based on split ring microwave resonators," *Sci. Rep.*, vol. 10, no. 1, Jul. 2020, Art. no. 12980.

[54] G. Ekinci, A. Calikoglu, S. N. Solak, A. D. Yalcinkaya, G. Dundar, and H. Torun, "Split-ring resonator-based sensors on flexible substrates for glaucoma monitoring," *Sensors Actuators A, Phys.*, vol. 268, pp. 32–37, 2017.

[55] H. Choi et al., "Design and in vitro interference test of microwave noninvasive blood glucose monitoring sensor," *IEEE Trans. Microw. Theory Techn.*, vol. 63, no. 10, pp. 3016–3025, Oct. 2015.

[56] J. Kilpijärvi, J. Tolvanen, J. Juuti, N. Halonen, and J. Hannu, "A non-invasive method for hydration status measurement with a microwave sensor using skin phantoms," *IEEE Sensors J.*, vol. 20, no. 2, pp. 1095–1104, Jan. 2020.

[57] D. Andreuccetti, R. Fossi, and C. Petrucci, "An internet resource for the calculation of the dielectric properties of body tissues in the frequency range 10 Hz–100 GHz," 1996. [Online]. Available: http://niremf.ifac.cnr.it/tissprop/

[58] S. Bing, K. Chawang, and J. C. Chiao, "A self-tuned method for impedance-matching of planar-loop resonators in conformable wearables," *Electronics*, vol. 11, no. 17, Sep. 2022, Art. no. 2784.

[59] S. Bing, K. Chawang, and J.-C. Chiao, "Sensitivity to limb curvatures for a non-invasive, conformal, planar resonant sensor," in *Proc. BMES Annu. Meeting*, 2021.

[60] J. Wei, "Distributed capacitance of planar electrodes in optic and acoustic surface wave devices," *IEEE J. Quantum Electron.*, vol. 13, no. 4, pp. 152–158, Apr. 1977.
[61] F. Maradei and S. Caniggia, *Appendix A: Formulae for Partial Inductance Calculation*. Chichester, U.K.: Wiley, Nov. 2008, pp. 481–486.
[62] S. Bing, K. Chawang, and J. C. Chiao, "A flexible tuned radio-frequency planar resonant loop for noninvasive hydration sensing," *IEEE J. Microwaves*, vol. 3, no. 1, pp. 181–192, Jan. 2023.
[63] S. Bing, K. Chawang, and J.-C. Chiao, "A radio-frequency planar resonant loop for noninvasive monitoring of water content," in *Proc. IEEE Sensors*, Dallas, TX, USA, Oct. 2022, pp. 1–4.
[64] G. Niu, S. Bing, B. Zhang, and J.-C. Chiao, "Particle filter-based diagnosis and prognosis for human hydration states," *IEEE Sens. Lett.*, vol. 7, no. 9, Sep. 2023, Art. no. 4502804.
[65] J. Chiao and S. Bing, "Noninvasive water content sensor," U.S. Patent 18/342,881, Jan. 11, 2024.
[66] S. Bing, K. Chawang, and J.-C. Chiao, "A resonant coupler for subcutaneous implant," *Sensors*, vol. 21, no. 23, Dec. 2021, Art. no. 8141.
[67] J. Chiao and S. Bing, "Resonant coupler systems and methods for implants," U.S. Patent 17/808,033, Dec. 22, 2022.
[68] S. Bing, K. Chawang, and J. C. Chiao, "A tuned microwave resonant system for subcutaneous imaging," *Sensors*, vol. 23, no. 6, Mar. 2023, Art. no. 3090.
[69] S. Bing and J.-C. Chiao, "A planar conformal microwave resonator for subcutaneous imaging," in *Proc. IEEE Int. Symp. Antennas Propag. USNC-URSI Radio Sci. Meeting*, Portland, OR, USA, 2023, pp. 335–336.
[70] S. Bing, K. Chawang, and J.-C. Chiao, "Planar conformal radio-frequency sensors for detection of tissue abnormity," in *Proc. Conf. Proc. Biol. Eng. Soc.*, 2022.
[71] S. Bing, K. Chawang, and J. C. Chiao, "A tuned microwave resonant sensor for skin cancerous tumor diagnosis," *IEEE J. Electromagn. RF Microw. Med. Biol.*, vol. 7, no. 4, pp. 320–327, Dec. 2023.
[72] S. Bing, K. Chawang, and J.-C. Chiao, "Resonant coupler designs for subcutaneous implants," in *Proc. IEEE Wireless Power Transfer Conf.*, 2021, pp. 1–4.
[73] S. Bing, K. Chawang, and J. C. Chiao, "A tuned microwave resonator on flexible substrate for nondestructive water content sensing in fruits," *IEEE J. Sel. Areas Sensors*, vol. 1, pp. 93–104, 2024.
[74] K. Mukai et al., "Factors affecting superficial vein visibility at the upper limb in healthy young adults: A cross-sectional observational study," *J. Vasc. Access*, vol. 21, no. 6, pp. 900–907, Nov. 2020.
[75] A. Chandrashekar, J. Garry, A. Gasparis, and N. Labropoulos, "Vein wall remodeling in patients with acute deep vein thrombosis and chronic postthrombotic changes," *J. Thromb. Haemostasis*, vol. 15, no. 10, pp. 1989–1993, Oct. 2017.
[76] N. Labropoulos, K. Summers, I. Escotto, and J. Raffetto, "Saphenous vein wall thickness in age and venous reflux-associated remodeling in adults," *J. Vasc. Surg.. Venous Lymphat. Disord.*, vol. 5, no. 2, pp. 216–223, Mar. 2017.
[77] S. A. R. Naqvi, M. Manoufali, B. Mohammed, A. T. Mobashsher, D. Foong, and A. M. Abbosh, "In vivo human skin dielectric properties characterization and statistical analysis at frequencies from 1 to 30 GHz," *IEEE Trans. Instrum. Meas.*, vol. 70, 2021, Art. no. 6001710.
[78] H. N. Mayrovitz, S. Carson, and M. Luis, "Male-female differences in forearm skin tissue dielectric constant," *Clin. Physiol. Funct. Imag.*, vol. 30, no. 5, pp. 328–332, Sep. 2010.
[79] H. N. Mayrovitz, A. Grammenos, K. Corbitt, and S. Bartos, "Young adult gender differences in forearm skin-to-fat tissue dielectric constant values measured at 300 MHz," *Skin Res. Technol.*, vol. 22, no. 1, pp. 81–88, Feb. 2016.
[80] G. Maenhout, T. Markovic, I. Ocket, and B. Nauwelaers, "Effect of open-ended coaxial probe-to-tissue contact pressure on dielectric measurements," *Sensors*, vol. 20, no. 7, Apr. 2020, Art. no. 2060.
[81] X. Feng, G.-Y. Li, A. Ramier, A. M. Eltony, and S.-H. Yun, "In vivo stiffness measurement of epidermis, dermis, and hypodermis using broadband rayleigh-wave optical coherence elastography," *Acta Biomaterialia*, vol. 146, pp. 295–305, Jul. 2022.
[82] A. F. Ghouri, W. Mading, and K. Prabaker, "Accidental intraarterial drug injections via intravascular catheters placed on the dorsum of the hand," *Anesth. Analg.*, vol. 95, no. 2, pp. 487–491, Aug. 2002.
[83] B. Scheer, A. Perel, and U. J. Pfeiffer, "Clinical review: Complications and risk factors of peripheral arterial catheters used for haemodynamic monitoring in anaesthesia and intensive care medicine," *Crit. Care*, vol. 6, no. 3, pp. 199–204, Jun. 2002.
[84] K. J. Chin and K. Singh, "The superficial ulnar artery–A potential hazard in patients with difficult venous access," *Brit. J. Anaesth.*, vol. 94, no. 5, pp. 692–693, May 2005.
[85] E. J. Yang, H. S. Ha, Y. H. Kong, and S. J. Kim, "Ultrasound-guided internal jugular vein catheterization in critically ill pediatric patients," *Clin. Exp. Pediatrics*, vol. 58, no. 4, pp. 136–141, Apr. 2015.
[86] M. Rodríguez-Niedenführ, T. Vázquez, L. Nearn, B. Ferreira, I. Parkin, and J. R. Sañudo, "Variations of the arterial pattern in the upper limb revisited: A morphological and statistical study, with a review of the literature," *J. Anatomy*, vol. 199, no. 5, pp. 547–566, Nov. 2001.
[87] P. Lirk et al., "Unintentional arterial puncture during cephalic vein cannulation: Case report and anatomical study," *Brit. J. Anaesth.*, vol. 92, no. 5, pp. 740–742, May 2004.
[88] N. L. Moureau, *Vessel Health and Preservation: The Right Approach for Vascular Access*, 1st ed. Cham, Switzerland: Springer, 2019.
[89] L. Gorski et al., *Infusion Therapy Standards of Practice*, 8th ed. Norwood, MA, USA: Infusion Nurses Society, Jan. 2021.
[90] C. Lake and C. L. Beecroft, "Extravasation injuries and accidental intra-arterial injection," *Continuing Educ. Anaesth. Crit. Care Pain*, vol. 10, no. 4, pp. 109–113, Aug. 2010.
[91] V. Shivappagoudar and B. George, "Unintentional arterial cannulation during cephalic vein cannulation," *Indian J. Anaesth.*, vol. 57, no. 3, pp. 320–322, May 2013.
[92] G. Borrego-Soto, R. Ortiz-López, and A. Rojas-Martínez, "Ionizing radiation-induced dna injury and damage detection in patients with breast cancer," *Genet. Mol. Biol.*, vol. 38, no. 4, pp. 420–432, Dec. 2015.
[93] A. B. Miller et al., "Risks to health and well-being from radio-frequency radiation emitted by cell phones and other wireless devices," *Front. Public Health*, vol. 7, Aug. 2019, Art. no. 223.
[94] FCC radio frequency (RF) safety faq. Accessed: Mar. 2024. [Online]. Available: https://www.fcc.gov/engineering-technology/electromagnetic-compatibility-division/radio-frequency-safety/faq/rf-safety
[95] I. International Commission on Non-Ionizing Radiation Protection, "Guidelines for limiting exposure to electromagnetic fields (100 KHz to 300 GHz)," *Health Phys.*, vol. 118, no. 5, pp. 483–524, May 2020.

SEN BING (Member, IEEE) received the B.Tech. degree in electronics and information science and technology from Hainan Normal University, Haikou, China, in 2017, and the M.S. degree in electrical engineering from Southern Methodist University, University Park, TX, USA, in 2019, where he is currently working toward the Ph.D. degree in electrical and computer engineering. He has authored or coauthored 13 journal articles and 14 conference papers on noninvasive wearable biomedical RF sensors, RF optimizing performance, wireless implants, factors affecting pH performance, and ultrasound medical imaging. His research interests include microwave biomedical devices, electrochemical biosensors, wearable electronics, medical imaging, RF devices, antenna design and medical signal analysis.

KHENGDAULIU CHAWANG (Graduate Student Member, IEEE) received the Bachelor of Technology degree in electronics and communication engineering from the National Institute of Technology, India, in 2012, and the Master of Science degree in electrical engineering from the University of Texas at Arlington, Arlington, TX, USA, in 2019. She is currently working toward the Ph.D. degree in electrical and computer engineering with Southern Methodist University, Dallas, TX. She has authored or coauthored seven conference papers on factors affecting pH performance. Her research interests include flexible and ultra-flexible devices by micro and nano fabrication, electrochemical biosensors, wearable electronics, and RF devices.

J.-C. CHIAO (Fellow, IEEE) received the B.S. degree from the Electrical Engineering Department, National Taiwan University, Taipei, Taiwan, in 1988, and the M.S. and Ph.D. degrees in electrical engineering from the California Institute of Technology, Pasadena, CA, USA, in 1991 and 1995, respectively. He was a Research Scientist with Optical Networking Systems and Testbeds Group, Bell Communications Research, an Assistant Professor of electrical engineering with the University of Hawaii, Honolulu, HI, USA, and Product Line Manager and Senior Technology Advisor with Chorum Technologies. He was Janet and Mike Greene endowed Professor and Jenkins Garrett Professor of electrical engineering with the University of Texas at Arlington, Arlington, TX, USA, from 2002 to 2018. He is currently a Mary and Richard Templeton Centennial Chair Professor of electrical and computer engineering with Southern Methodist University, Dallas, TX, USA. He has authored or coauthored and edited numerous peer-reviewed technical journal and conference papers, book chapters, proceedings and books. He holds 20 patents in RF MEMS, MEMS optical, liquid crystal, nano-scale fabrication, and wireless medical sensor technologies. His research works have been covered by media extensively including *Forbes*, *National Geographic* magazine, National Public Radio and CBS Henry Ford Innovation Nation. Dr. Chiao is the Chair and Technical Program Chair of several international conferences including 2018 IEEE International Microwave Biomedical Conference (IMBioC) and 2021 IEEE Wireless Power Transfer Conference. He was the Chair of the IEEE MTT-S Technical Committee 10 "Biological Effect and Medical Applications of RF and Microwave," and an Associate Editor for IEEE TRANSACTIONS ON MICROWAVE THEORY AND TECHNIQUES. He was the founding Editor-in-Chief of the IEEE JOURNAL OF ELECTROMAGNETICS, RF, AND MICROWAVES IN MEDICINE AND BIOLOGY. He is with the Editorial Board of IEEE ACCESS and Track Editor of IEEE JOURNAL OF MICROWAVES. He was the recipient of the Lockheed Martin Aeronautics Company Excellence in Engineering Teaching Award, Tech Titans Technology Innovator Award, Research in Medicine award in the Heroes of Healthcare, IEEE Region 5 Outstanding Engineering Educator award, IEEE Region 5 Excellent Performance award, 2012−2014 IEEE MTT Distinguished Microwave Lecturer, 2017−2019 IEEE Sensors Council Distinguished Lecturer, Pan Wen-Yuan Foundation Excellence in Research Award, and the 2011 Edith and Peter O'Donnell Award in Engineering by The Academy of Medicine, Engineering and Science of Texas. He is a Fellow of IET, SPIE, AIMBE, AAIA and NAI.